

Parallel TreeSPH

Romeel Davé, John Dubinski¹, and Lars Hernquist²
 Astronomy Dept., University of California, Santa Cruz, CA 95064

ABSTRACT

We describe PTreeSPH, a gravity treecode combined with an SPH hydrodynamics code designed for massively parallel supercomputers having distributed memory. Our computational algorithm is based on the popular TreeSPH code of Hernquist & Katz (1989). PTreeSPH utilizes a domain decomposition procedure and a synchronous hypercube communication paradigm to build self-contained subvolumes of the simulation on each processor at every timestep. Computations then proceed in a manner analogous to a serial code. We use the Message Passing Interface (MPI) communications package, making our code easily portable to a variety of parallel systems. PTreeSPH uses individual smoothing lengths and timesteps, with a communication algorithm designed to minimize exchange of information while still providing all information required to accurately perform SPH computations. We have additionally incorporated cosmology, periodic boundary conditions with forces calculated using a quadrupole Ewald summation method, and radiative cooling and heating from a parameterized ionizing background following Katz, Weinberg & Hernquist (1996). The addition of other physical processes, such as star formation, is straightforward. A cosmological simulation from $z = 49$ to $z = 2$ with 64^3 gas particles and 64^3 dark matter particles requires ~ 6000 node-hours on a Cray T3D, with a communications overhead of $\sim 10\%$ and is load balanced to a $\sim 90\%$ level. When used on the new Cray T3E, this code will be capable of performing cosmological hydrodynamical simulations down to $z = 0$ with $\sim 2 \times 10^6$ particles, or to $z = 2$ with $\sim 10^7$ particles, in a reasonable amount of time. Even larger simulations will be practical in situations where the matter is not highly clustered or when periodic boundaries are not required.

Subject Headings: methods: numerical — cosmology: theory

¹Current address: CITA, Univ. of Toronto, 60 St. George St., Toronto, Ontario M5S 1A7, Canada

²Presidential Faculty Fellow

1. Introduction

Gas dynamics and gravitational forces together govern the evolution of astrophysical systems on nearly all scales. Star and planet formation are thought to occur in accretion disks well-represented as collapsing gas clouds in quasi-hydrostatic equilibrium. The formation and evolution of star clusters is governed by interactions with the interstellar medium, as well as viscous forces generated from tidal perturbations in individual stellar interactions. Shock heating from supernovae feedback is important for the observed structure of galaxies and the creation of hot X-ray halos around clusters. All the galaxies we see are themselves thought to have resulted from dissipational collapse through hierarchical gravitational instability. On these largest scales, comparison between observation and theory requires some understanding of the interplay between dissipationless dark matter and baryonic material.

Analytical treatments of the processes relevant to cosmology are generally applicable only when the matter is still evolving in a linear or quasi-linear fashion, or more generally for objects possessing inherent symmetries such as stars, supernovae, or accretion disks. However, many systems are intrinsically asymmetric and/or highly nonlinear, such as galaxies forming from primordial fluctuations. Semi-analytical treatments of galaxy formation invariably make *ad hoc* assumptions about the relationships between gas and dark matter in the highly nonlinear regime (*e.g.* Kauffmann & White 1993; Heyl et al. 1995; Somerville et al. 1997). A proper understanding of galaxy and structure formation requires that dissipation, shocks, and pressure forces be taken into account, in addition to gravitational collapse.

Highly nonlinear systems are best modelled numerically by evolving large numbers of particles and/or grid cells self-consistently under both gravitational and hydrodynamical forces. A variety of techniques to do this have been developed, each with its own advantages and disadvantages. Gravitational forces are computed using either grid-based or particle-based algorithms. The simplest particle-based technique directly sums pairwise forces between all particle pairs. These codes are useful for many purposes (*e.g.* Aarseth 1985), but the computational time grows with particle number N as $O(N^2)$ or worse, making them appropriate only for small systems ($N \lesssim 10^4$). Tree codes place particles in a hierarchical data structure, and use multipole expansions to approximate the force between distant groups of particles, reducing the scaling to $O(N \log N)$ (*e.g.* Barnes & Hut 1986, hereafter BH). In particle-mesh (PM) codes, the gravitational potential is computed on a grid using Fast Fourier Transforms (FFTs), which also scales as $O(N \log N)$ but with fewer operations than a treecode (*e.g.* Hockney & Eastwood 1980). The main drawback of this approach is that the resolution is limited by the cell size. Adaptive mesh codes have been developed to subdivide or deform cells in dense regions to obtain better dynamic range (Villumsen 1989; Pen 1995; Xu 1997). Also, hybrid codes such as PP-PM (P³M; Efstathiou et al. 1985) and Tree-PM (TPM; Xu 1995) alleviate resolution limitations. Other techniques,

such as the self-consistent field (SCF) method (*e.g.* Hernquist & Ostriker 1992) can be even faster, but are generally useful only for systems not far from a well-specified equilibrium.

Hydrodynamical forces can be computed in either a Lagrangian or Eulerian manner. Eulerian codes represent the fluid on a grid of cells, and compute the flux of fluid across cell boundaries, as in the Piecewise Parabolic Method (PPM) (Colella & Woodward 1984; Bryan et al. 1994). In Lagrangian codes, the dynamical equations are obtained from the Lagrangian form of the hydrodynamical conservation laws. Some Lagrangian codes represent the fluid by particles without the use of a grid, as in Smoothed Particle Hydrodynamics (SPH) (Lucy 1977; Gingold & Monaghan 1977).

In principle, any gravity solver may be combined with any hydrodynamics method. Grid-based codes include PM-PPM (Bryan et al. 1994), PM-TVD (Ryu et al. 1993), and adaptive mesh hydrodynamics codes (*e.g.* Bryan & Norman 1995). Lagrangian examples include P³M-SPH (Evrard 1988; Couchman, Thomas & Pearce 1995), and GRAPE-SPH (Steinmetz 1996), which uses the special-purpose GRAPE hardware to perform rapid pairwise gravity summation. Lagrangian codes provide much better spatial resolution in high density regions compared with Eulerian codes for a given computational expense, at the cost of poorer shock resolution and lower resolution in underdense regions (Kang et al. 1994). For many astrophysical applications the overdense regions are of most immediate interest, and in those cases Lagrangian codes are preferable if shocks do not dominate the dynamics of the system.

In this paper we focus on a pure particle-based combination of gravity and hydrodynamics solvers analogous to the TreeSPH code of Hernquist & Katz (1989; hereafter HK). In SPH, the gas is sampled and represented by particles, which are smoothed to obtain a continuous distribution of gas properties. Since there is no grid, there are no inherent constraints on the global geometry or spatial resolution. Neighbor finding is also done using a tree structure, and thus the entire code scales as $\sim O(N \log N)$. However, unlike grid-based codes, SPH cannot handle arbitrarily large gradients due to its finite particle resolution. Also, an artificial viscosity is used to capture shocks, further limiting the spatial resolution locally. Despite these compromises, TreeSPH has been successfully used in a wide range of astrophysical applications, including giant molecular clouds (Gammie 1992), colliding galaxies (Mihos & Hernquist 1994), ram pressure stripping in clusters (Kundic, Spergel & Hernquist 1993), formation of galaxies (Katz & Gunn 1991) and cluster (Katz & White 1993), and the high-redshift Lyman alpha forest (Hernquist et al. 1996).

A major goal in numerical astrophysics is to improve the dynamic range of simulations. One would ideally like to simulate volumes comparable to the size of the Universe ($\sim 10^3$ Mpc), but resolve star forming regions in galaxies on the parsec scale. The spatial dynamical range required per dimension is thus $\sim 10^9$, well beyond the $\sim 10^3$ in dynamic range that codes can currently achieve. High resolution studies of

even single collapsing protogalaxies in a cosmological setting require a dynamic range $\gtrsim 10^4$. TreeSPH endows each gas particle with its own smoothing length and timestep, thus improving the dynamic range substantially by being adaptive in both space and time. TreeSPH has been vectorized efficiently (HK; Hernquist 1990), but even on vector supercomputers the largest TreeSPH cosmological simulation to date (Katz, Weinberg & Hernquist 1996, hereafter KWH) employed a total of $\approx 524,288$ particles with a dynamic range of ~ 2000 .

Massively parallel supercomputers (MPPs) link hundreds of workstation processors together to yield an overall computational power more than an order of magnitude greater than that of current vector supercomputers. While MPPs are attractive, there are a number of major difficulties in adapting codes to run on these machines, often requiring significant algorithmic changes from serial or vector code. The first difficulty is that in distributed memory systems, each processor possesses only a relatively small amount of local memory, and accessing information from another processor’s memory is slow compared to the computation speed. Thus a parallel code must subdivide a simulation and exchange information between processors in a manner which minimizes communication time, while not taxing each processor’s memory. The second complication is *load balancing*, *i.e.* insuring that no processor spends a significant amount of time idly waiting for another processor to send required information. Good load balancing can be achieved either by designing an algorithm so that each processor has roughly an equal amount of computational work between *synchronous* communications, or by implementing an *asynchronous* communication scheme by which processors continue to do other computations while waiting to send or receive information.

In this paper we present a parallel implementation of a gravitational treecode combined with SPH, called PTreeSPH. While the underlying numerical techniques are similar to those in TreeSPH, our implementation on MPP machines required a complete redesign of the code as well as several major algorithmic changes. PTreeSPH is a *C* code which uses a domain decomposition prescription to subdivide the simulation and a synchronous hypercube message-passing paradigm to build small “locally essential” simulation subvolumes on each processor. The *N*-body portion of the code was developed by Dubinski (1996; hereafter Paper I), to which we have added a parallelized version of SPH as well as the dynamics required for cosmological simulations. Building locally essential simulations on each processor allows the parallelization to be decoupled from the computations, making it straightforward to incorporate additional physical processes. In addition, information transfers occur in single bursts rather than continually during a simulation, thereby lowering communication overhead. We utilize the Message Passing Interface (MPI) package exclusively to handle processor communications, which makes the code easily portable to most major parallel supercomputers, including the Cray T3D/T3E, IBM SP2, and

Intel Paragon, shared memory systems such as the SGI Power Challenge, as well as to networks of workstations. While our parallel algorithm could likely be made more efficient by tailoring it to specific machines and including some asynchronous communication, we are more interested in producing a reasonably efficient code which is portable and adaptable to a wide variety of applications.

Several other groups are now parallelizing SPH in various forms. The Virgo Consortium has recently developed a parallel P³M-SPH code capable of doing cosmological simulations (Pearce et al. 1995; Jenkins et al. 1996). Evrard and Brieu (private communication) are working on a similar code. Warren & Salmon (1994) have developed a generalized parallel N -body code using a hashed octal tree structure to asynchronously access information on other processors, and they describe how their code may be applied to neighbor finding as required in SPH. Also, Dikaiakos & Stadel (1997) have written a parallel N -body treecode similar in spirit to Warren & Salmon (1994), and are now adding their own parallel version of SPH to it.

2. The Parallel N -Body Treecode

2.1. The Barnes-Hut Treecode

Paper I fully describes Dubinski’s implementation of a parallel treecode, which is based on Salmon’s (1990) algorithm. It uses the BH method of tree construction, by which the simulation volume is subdivided recursively into equal-sized octants, called *cells*. If there is only a single particle in a given cell, that cell is not further subdivided. The data structure is then a tree, with the *root cell* at the top, and successively smaller cells at each level. The mass distribution within a cell is approximated as a multipole truncated typically at quadrupole order (*e.g.* Hernquist 1987). The force on any given particle is then the sum of the (exact) force from nearby particles, plus the force from distant cells approximated as multipoles. The criterion for approximating cells as a multipole is given by the *opening criterion*:

$$d > \frac{l}{\theta} + \delta \tag{1}$$

where d is the distance from the particle to the cell’s center of mass, l is the longest edge of the cell, δ is the distance between the cell’s center of mass and its geometric center, and θ is a user-defined parameter that gives greater accuracy when smaller. This opening criterion, introduced by Barnes (1994), avoids numerical pathologies from highly skewed distributions within a cell. For $\theta \approx 1.0$ at quadrupole order, the median error is roughly 0.7%. Dubinski also improved efficiency by using grouping and a non-recursive treewalk using a linked list of tree cells (see Paper I for details).

2.2. Domain Decomposition and Locally Essential Trees

To parallelize a particle simulation, one must have an algorithm to assign particles to processors. Paper I used the intuitive *domain decomposition* method, whereby a given processor handles all the particles within a rectangular subvolume of the system. A treecode naturally lends itself to such a decomposition, since the processors can be assigned to be cells in an overall tree (see Paper I: fig. 4). However, mapping the equal-sized subvolumes inherent in the Barnes-Hut tree structure onto individual processors does not lend itself to optimal load balancing, especially in clustered simulations typical of gravitational collapse, because clustered subvolumes require more computational time than unclustered subvolumes. Salmon (1991) solved this problem by tracking the “work” done by each particle (*i.e.* the number of floating point operations required to compute the force of each particle), and using that information to subdivide the simulation into volumes of roughly equal computational work (rather than equal volume) at the next timestep. This produces an ORB (orthogonal recursive bisection) load-balanced processor tree. Initially, all particles are assumed to require equal work and the simulation may not be well load-balanced, but within a few timesteps the load balancing becomes quite satisfactory (Paper I: Table 1). On each individual processor, a Barnes-Hut tree is constructed and appended below ORB tree.

To perform a force calculation, a given processor’s particles need information from trees on other processors. However, each processor cannot maintain a full copy of every other processor’s tree structure due to memory constraints. Instead, each processor builds its own *locally essential tree*, *i.e.* the portion of the entire simulation’s tree which is required for all the local particles’ force computations. The method for doing this is described in Paper I, and the reader is referred there for details. The central idea is that after all the parallel manipulations and communications, each processor contains a tree structure which is sufficiently complete to perform all its local particles’ gravitational force computations, and no further communication is required to compute the gravitational accelerations for that timestep.

2.3. Periodic Boundaries using Ewald Summation

Dubinski (1997) has recently implemented a cosmological version of the parallel tree code using the Ewald method (Ewald 1921; Hernquist, Bouchet & Suto 1991, hereafter HBS). Cosmological N -body simulations are typically run in a cube with periodic boundaries in a comoving coordinate system (Efstathiou et al. 1985). While the periodicity is a natural property of FFT based codes, it must be imposed in a treecode by replacing the usual Newtonian gravitational potential of a particle (or cell) with the potential of the infinite, periodic lattice of image particles (or cells). The potential of the images can be represented accurately using Ewald’s method which replaces the single, slowly converging sum for the images with two, rapidly converging

sums which can be truncated at a small number of terms. In practice, the tree descent is modified so that the distance to a cell used in the cell-opening criterion is the minimum of the distance to the cell within the simulation cube and the nearest image cell, *i.e.* $\delta\mathbf{r} = [\min(\delta x, L - \delta x), \min(\delta y, L - \delta y), \min(\delta z, L - \delta z)]$, where L is length of the cube. The potential from a cell is taken as the sum of the Newtonian potential as calculated by the treecode plus a correction term from the lattice of images. Since the correction terms are relatively expensive to calculate, we calculate them on a grid prior to the simulation and then use bi-linear interpolation to determine the correction terms as needed. In HBS and TreeSPH, the correction terms are only calculated to monopole order forcing the use of a small opening-angle parameter. In PTreeSPH, we calculate the quadrupole order Ewald correction term as well for particle-cell interactions allowing larger values of the opening angle parameter and more accurate forces. It is too costly to use bilinear interpolation for the quadrupole terms but since they are smaller corrections it is sufficient to use nearest grid point table lookups for these terms. The calculation of Ewald corrections slows down the code generally by a factor of two for a given number of particle-cell interactions. Typical code speeds on the T3D for the gravity portion are therefore between ~ 100 – 200 particles/s/processor depending on the value of θ .

The acceleration errors, $\delta a/a$, associated with the Ewald method tend to be large in the linear regime for a given opening angle parameter θ . In a 32K particle CDM test simulation, the errors for $\theta = 0.5(0.7)$ are as large as 10%(30%) at monopole order and 2.5%(7%) at quadrupole order in the linear regime. Furthermore, the accelerations are systematically overestimated, so when θ is too large particles can be pushed too swiftly through the linear regime with consequences that will be outlined in §4.3. Once the particles become clustered, the errors are much smaller with $\delta/a = 0.2\%(1.1\%)$ for $\theta = 0.7(1.0)$ both to quadrupole order. We therefore use $\theta = 0.4$ in the linear and weakly clustered regime, growing with the expansion factor up to $\theta = 0.8$. Once the particles are strongly clustered, a value of $\theta = 0.8$ gives accelerations with $\sim 0.7\%$ accuracy. Quadrupole order corrections are used at all times.

We have compared the Ewald tree code to two other N -body codes: TPM (Xu 1995) and an adaptive particle mesh (APM) code (Couchman, Thomas & Pearce 1995). The results of a 2 million particle CDM simulation using TPM and our code agree very well. The density profiles of the ten largest virialized clusters in the simulation are nearly identical. The only noticeable differences are in the positions of the small satellites in orbit around larger dark halos. This might be expected since bound orbits diverge chaotically in the presence of small differences in the acceleration brought on by random variations. A comparison of the formation of a cluster in a 256K particle simulation with Couchman’s code also showed good agreement. The cluster density profiles again are nearly identical.

2.4. Performance Characteristics

Ideally, the wall-clock time required by a parallel code should scale precisely as the inverse of the number of processors employed. In practice this perfect scalability cannot be achieved because communications and the overhead associated with locally essential tree building increase with the number of processors. Therefore it is desirable to place as large a number of particles on each processor as memory constraints will allow, so that computation time versus communication time is maximized. On a Cray T3D with 8 Megawords per processor, this translates to over 100K N -body particles. However, even down to 16K particles per processor Dubinski’s treecode barely suffers a few percent loss in speed from the ideal (Paper I: fig. 7), showing good scaling and load balancing. The total communication overhead is also small, being less than 5% for fully-loaded processors (Paper I: Table 1; see also §5.1 and Table 5.1).

3. Parallelizing SPH

3.1. General Overview of SPH

Smoothed Particle Hydrodynamics (see Monaghan 1992 for a review) uses locally averaged hydrodynamical quantities to estimate properties associated with individual particles. Each particle is smoothed with a kernel, typically a Gaussian or spline, over a range of several *smoothing lengths*. Gas properties for individual particles are then estimated by summing over nearest neighbors, as in

$$\begin{aligned} \rho_i &= \sum_j m_j W(\mathbf{x}_i - \mathbf{x}_j, h_i, h_j), \\ \frac{d\mathbf{v}}{dt} = -\frac{1}{\rho}\nabla P &\implies \frac{d\mathbf{v}_i}{dt} = -\sum_j m_j \left(2\frac{\sqrt{P_i P_j}}{\rho_i \rho_j} + \Pi_{ij} \right) \nabla_i W, \text{ and} \\ \frac{du}{dt} = -\frac{P}{\rho}\nabla \cdot \mathbf{v} &\implies \frac{du_i}{dt} = -\frac{1}{\rho_i} \sum_j m_j \left(\frac{\sqrt{P_i P_j}}{\rho_i \rho_j} + \frac{1}{2}\Pi_{ij} \right) (\mathbf{v}_i - \mathbf{v}_j) \cdot \nabla_i W, \end{aligned} \quad (2)$$

where h_i is the smoothing length, adjusted to keep a constant number of neighbors N_{smooth} within $2h_i$, and m_i , \mathbf{v}_i , ρ_i , P_i , and u_i are the mass, velocity, density, pressure, and specific thermal energy associated with each particle. For the kernel function W , we take a spline function with compact support within a radius of $2h_i$ given by (Monaghan & Lattanzio 1985)

$$W(r, h) \equiv \frac{1}{\pi h^3} \begin{cases} 1 - 1.5(r/h)^2 + 0.75(r/h)^3 & 0 \leq r/h < 1, \\ 0.25[1 - (r/h)]^3 & 1 \leq r/h < 2, \\ 0 & r/h \geq 2, \end{cases} \quad (3)$$

then take the average over particles i and j according to HK

$$W(\mathbf{x}_i - \mathbf{x}_j, h_i, h_j) = \frac{1}{2}[W(\mathbf{x}_i - \mathbf{x}_j, h_i) + W(\mathbf{x}_i - \mathbf{x}_j, h_j)]. \quad (4)$$

In equation (2), Π_{ij} is the artificial viscosity given by

$$\Pi_{ij} = \frac{q_i}{\rho_i^2} + \frac{q_j}{\rho_j^2}, \quad (5)$$

with

$$q_i = \begin{cases} \alpha h_i \rho_i c_i |\nabla \cdot \mathbf{v}|_i + \beta h_i^2 \rho_i |\nabla \cdot \mathbf{v}|_i^2 & \text{for } |\nabla \cdot \mathbf{v}|_i < 0 \\ 0 & \text{for } |\nabla \cdot \mathbf{v}|_i \geq 0 \end{cases} \quad (6)$$

Additionally, we set $\Pi_{ij} = 0$ for particle i if $\mathbf{v}_i \cdot \mathbf{x}_i \geq 0$. The parameters $\alpha \approx \beta \approx 0.5$ are user-defined parameters which add dissipation in the presence of shocks. The use of symmetrized quantities insures momentum conservation. The version of SPH used here is quite similar to the one in HK and KWH. Other choices are possible for various aspects of the SPH calculations, in particular for the smoothing procedure and for the artificial viscosity (see *e.g.* HK and Monaghan 1992).

We incorporate an optional lower limit on the smoothing length, specified as some fraction (typically 1/4) of the gravitational softening length ϵ_{grav} (Evrard 1988). This only has an effect on scales smaller than ϵ_{grav} which are unresolved anyway, but prevents the use of very small timesteps which slows the calculation.

A single TreeSPH timestep, from t^n to t^{n+1} , proceeds as follows:

- Begin with $\mathbf{x}^n, \mathbf{v}^n, u^n$ at t^n .
- Advance $\mathbf{x}^n \rightarrow \mathbf{x}^{n+1/2}$ using \mathbf{v}^n .
- Compute $\mathbf{a}_{\text{grav}}^{n+1/2}$ using $\mathbf{x}^{n+1/2}$.
- Estimate $\hat{\mathbf{v}}^{n+1/2}$ using $\mathbf{a}^{n-1/2}$
- Determine $h^{n+1/2}$ using $\mathbf{x}^{n+1/2}$ by requiring N_{smooth} neighbors.
- Compute $\rho^{n+1/2}$ using $\mathbf{x}^{n+1/2}$ and $h^{n+1/2}$.
- Advance $u^n \rightarrow u^{n+1/2}$ by a semi-implicit scheme (see §3.9 below).
- Compute $\mathbf{a}_{\text{hydro}}^{n+1/2}$ using $\mathbf{x}^{n+1/2}, h^{n+1/2}, u^{n+1/2}$ and $\hat{\mathbf{v}}^{n+1/2}$.
- Advance $\mathbf{v}^n \rightarrow \mathbf{v}^{n+1}$ using $\mathbf{a}_{\text{total}}^{n+1/2}$.
- Advance $\mathbf{x}^{n+1/2} \rightarrow \mathbf{x}^{n+1}$ using \mathbf{v}^{n+1} .
- Advance $u^{n+1/2} \rightarrow u^{n+1}$ by a semi-implicit scheme (§3.9).

The use of time-centered quantities maintains errors at $O(\Delta t^2)$. The parallelization of this algorithm is the focus of the remainder of this section.

3.2. Parallelization Strategy

A parallel implementation of SPH must be able to detect and compute the contribution to SPH sums from neighboring particles j which can be on different processors from particle i . There are various strategies to handle this problem.

The simplest method is to obtain information from another processor whenever it is required; however, the communication overhead is prohibitive because a single processor must idly wait for the other processor to pass along the information when it becomes ready, and there is usually significant overhead in establishing interprocessor communication. This problem can be alleviated by using asynchronous communication, by which a given processor continues to perform other work while waiting for information. In PTreeSPH, we adopt an alternate strategy of using synchronous communications to build a *locally essential particle list* (LEPL), a collection of all particles from other processors required to perform the local processor’s SPH computations. The second difficulty arises because the LEPL (obtained at the beginning of each timestep) contains information updated to the previous timestep, whereas SPH sums require current timestep information. Thus we have developed a request-send algorithm to update gas particle information during the timestep using the minimum possible amount of communication. Communication benchmarks for our approach are comparable to those of the asynchronous code presented in Warren & Salmon (1994).

To properly load-balance by the equal-work scheme, one must keep track of the computational work done for each SPH particle. This turns out to be much more complicated than in the case of gravity alone where there is a single computation (particle-cell interaction) which takes the bulk of the time. Thus we simply neglect this issue for now; that is, we use the same particle list from the N -body domain decomposition, and compute the pressure forces on the subset of those which are SPH particles. It turns out that the SPH load balancing is still quite good (see §5.1 and Table 5.1), which is not surprising considering that denser regions will tend to be more computationally expensive for both gravity and SPH.

3.3. Building the Locally Essential Particle List

The locally essential particle list (LEPL) is at the heart of our parallel implementation of SPH. By collecting a complete list of particles required for a local SPH computation, we effectively isolate the parallel portion of the code from the computation of physical quantities, in a manner analogous to the locally essential trees in the N -body portion.

In the case of building the locally essential trees, each processor obtains the spatial extent of every other processor and therefore is able to use the opening criterion to determine the tree information required by every other processor. For the LEPL, the situation is more complicated, as the particle information required depends sensitively on the (often highly variable) smoothing region of particles near a given processor’s boundary. Obtaining all particles within the maximum extent of a processor’s smoothing region was found to be prohibitive in both communication time

and memory, requiring large numbers of unnecessary particles to be transmitted and stored. Instead, we have developed an algorithm by which each processor obtains only those particles required for the LEPL from the other processors, and no (or very few) more.

The SPH formalism of HK averages the gather and scatter kernels to insure symmetry of forces between every pair of particles, thereby conserving momentum. Thus the algorithm must perform both a *gather search* to obtain all non-local particles which fall within a local particle’s smoothing region, and a *scatter search* to find all the non-local particles whose smoothing regions enclose local particles. In all operations, only gas particles are considered, while dark matter particles are ignored.

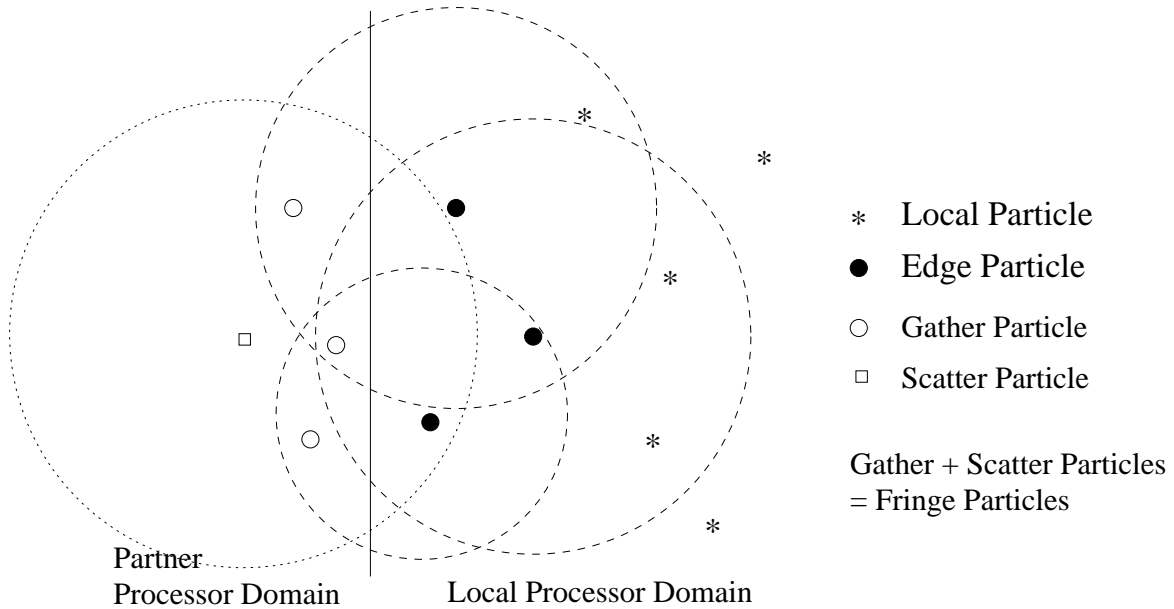


Fig. 1.— A locally essential particle list (LEPL). Most local particles (asterisks) require no information from other processors. Edge Particles (filled circles), however, have smoothing volumes which extend into the neighboring processor’s domain. A search of Edge Particles’ smoothing volumes identifies the Gather particles (open circles). A scatter search must also be done to insure that the Scatter particles (open square) are identified as well. The Gather and Scatter particles together form the Fringe particles, which are then sent back to the local processor for use in computations. After all Fringe particles have been collected from every other processor, SPH computations may proceed analogously to a serial code, except when data updates are required.

The LEPL building algorithm (see Figure 1) proceeds simultaneously on every processor, with communications done synchronously with the partner processor when required.

- Identify particles whose search region extends into the partner processor’s domain, which we call Edge particles.

- Exchange Edge particles with partner processor. Now the local processor possesses a list of Partner Edge particles.
- Gather Search: For each Partner Edge particle, search and tag Fringe particles, *i.e.* local neighbors of Partner Edge particles.
- Scatter Search:
 - Tag all particles which are local Edge particles but have not already been tagged as Fringe particles.
 - Find maximum smoothing length of those particles.
 - For each Partner Edge particle, tag all particles within maximum scatter search region as Fringe particles.
- Exchange tagged Fringe particles with partner processor.
- Append the received Fringe particles to local particles to obtain the LEPL.

A given processor performs this procedure with every other processor in the simulation, although more distant processors will usually require no exchange of particles. This makes the communications scheme scale as N_P^2 , where N_P is the number of processors, which is not as optimal as the $N_P \log N_P$ scaling of the N -body parallelization. Upon completion, a given processor possesses a complete set of *Fringe particles*, which are all particles outside the local domain which overlap in either a gather or scatter mode with one of the local particles.

The scatter search is somewhat inefficient because it uses a maximum smoothing length, and often re-tags many of the particles already identified as Fringe particles. Nevertheless it uses a relatively small portion of the LEPL computation time, so we leave it for the future to improve this algorithm.

3.4. Data Updates

In SPH, the value computed for the density is subsequently used to compute du/dt and advance u , which in turn is used to compute $d\mathbf{v}/dt$. However, the LEPL contains only particle information updated to the previous timestep. Thus after each processor completes a computation, a *data update* must be done to obtain the current values of Fringe particle properties from other processors. Unlike with locally essential trees, communication must occur during the timestep as well as at the beginning.

To facilitate this, each gas particle carries not only an overall identification number, but also a *local* identification number, which is sequential on each processor. When received from another processor, a particle’s local ID is encoded with the number of its host processor. To update a physical quantity in a Fringe particle, we then use the following algorithm, again running on all processors simultaneously between synchronous communications:

- Collect a list of local IDs of particles which are in the partner processor’s domain.

- Exchange these *request IDs* between processors.
- Compile the required data for the list of request IDs.
- Exchange the requested data.
- Update the Fringe particles with the received data.

During each timestep, a data exchange is performed after any computation which recomputes physical quantities (density, smoothing length, etc.) for local particles. In this manner each processor always uses the most up-to-date information to compute smoothed averages of SPH quantities.

3.5. Variable Smoothing Lengths

Since smoothing lengths are varied to keep a fixed number of particles within each particle’s smoothing region, an algorithm must be used to guarantee that a given particle is obtaining all Fringe particles within its current smoothing region. Using the previous step’s smoothing length will lead to errors, since the smoothing length may very well increase at the current timestep and thus all Fringe particles will not be properly identified in the gather search.

At the first timestep, all smoothing lengths are adjusted to encompass N_{smooth} particles *within the local processor domain*. For interior particles, this smoothing length is the true smoothing length; for Edge particles, this smoothing length is guaranteed to be equal to or greater than the true smoothing length, since it will find less particles than actually exist within its search volume. Thus the LEPL will contain more Fringe particles than necessary. After building the LEPL, the smoothing length of Edge particles may be readjusted downwards to the correct value.

While this algorithm would work at all timesteps, the overcounting of Fringe particles reduces efficiency. To avoid this, we perform the following algorithm at the end of each timestep: First, a data update is performed to obtain all the Fringe particles’ current positions. Then the smoothing lengths of Edge particles are re-adjusted. This prediction will be much closer to the actual value since it includes Fringe particles (unlike at the first timestep), but is guaranteed to err on the side of undercounting the number of particles within the search region, and thus overestimating the smoothing length. After the slightly overestimated smoothing length is used in collecting the LEPL, once again it can be readjusted downwards to the proper value.

3.6. Grid-Tree Neighbor Searching

In TreeSPH, neighbors are accumulated once per timestep and stored in memory, then recalled for each sum; despite this, the CPU time taken for neighbor finding is typically $\sim 1/3$ of the entire simulation time. For parallel machines, storing a list of ~ 30 neighbors per particle is prohibitive, since code performance degrades with

increased memory usage (see §3.8). This necessitated the development of a significantly faster algorithm using a hybrid grid-tree data structure for neighbor finding. With grid-tree searching, neighbors can be found whenever needed (typically on six separate occasions during a timestep), thereby eliminating the need for storing neighbor lists in memory. Despite the repetition, the fraction of computation time required for neighbor finding is comparable to that in TreeSPH.

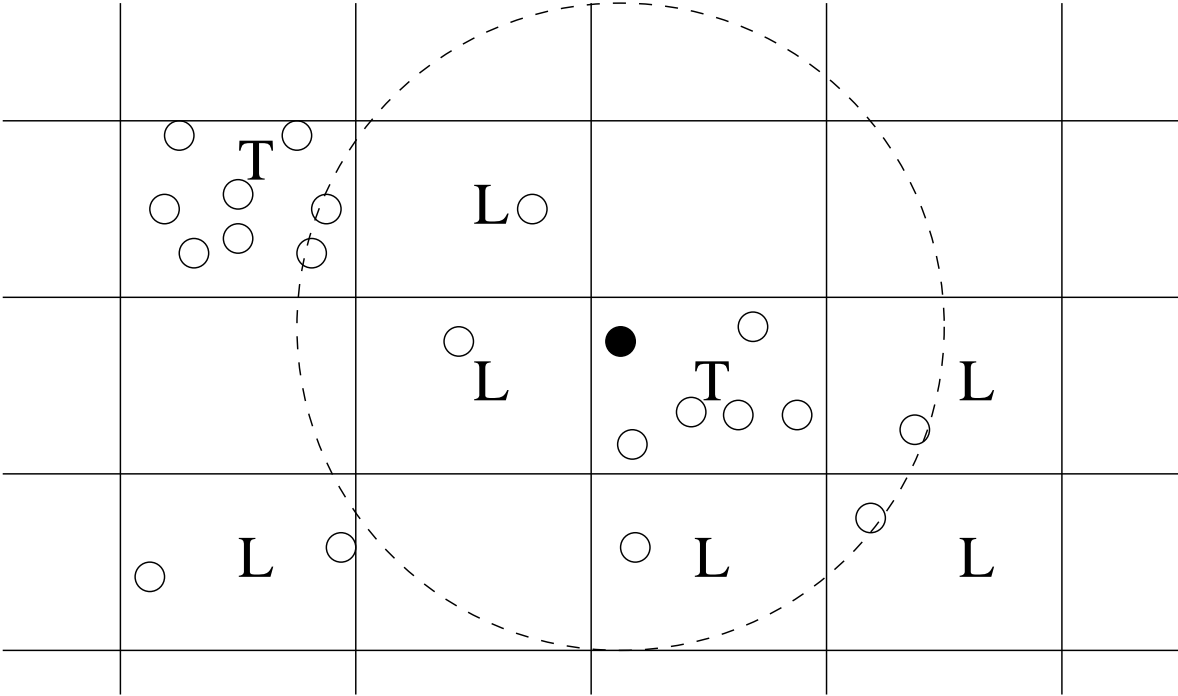


Fig. 2.— A schematic representation of the grid-tree data structure. In high-density grid cells (marked with a “T”) the particles within that cell are organized into a tree structure, while in lower-density grid cells (marked with a “L”) the particles are left as a linked list. When searching for neighbors, the algorithm performs a treewalk in the dense grid cells, and cycles through the linked list in less dense grid cells. Thus the worst-case (highly clustered) scaling remains at $O(N \log N)$, while most of the volume utilizes the faster grid-linked list search.

The grid-tree scheme combines a grid-linked list search with a tree search to obtain the speed advantages of both. A grid-linked list search bins particles onto a grid, then makes a linked list of particles within each grid cell. Searching is then done by first identifying which grid cells to search through, then cycling through each grid cell’s linked list and checking if each particle is within the search region. The grid-linked list search is up to five times faster than the tree search method when all particles have roughly the same smoothing length. However, since the search time scales as $O(N^2)$ where N is number in a densest grid cell, this method rapidly deteriorates in clustered situations typical of astrophysical applications.

A tree search walks down the tree by determining if the particle’s search region extends into a given tree cell. If so, the cell is “opened” into its subcells, and the test is repeated on the subcells, and so on until all neighbors are found. TreeSPH used a pure tree search, which scales as $O(N \log N)$ regardless of clustering.

In the grid-tree structure in PTreeSPH, we replace the linked list with a tree structure when the number of particles in a grid cell exceeds a threshold value, typically ~ 50 . The searching routines automatically detects whether a grid cell contains a tree or linked list, and performs the appropriate search (see Figure 2). In unclustered regions we achieve the benefits of a grid-linked list, while in clustered regions the search time still scales as $O(N \log N)$. For cosmologically clustered situations, typical speedup is a factor of $\gtrsim 2$.

By using the grid-tree scheme and writing the code in *C* (generally a faster language than FORTRAN when handling data structures), we have achieved relative speedups of factors of five over TreeSPH neighbor searching, removing the need to store neighbor lists.

3.7. Multiple Timestepping

PTreeSPH uses individual timesteps for all particles, thereby concentrating the computational effort in regions where higher resolution is required. For the dissipationless particles, we use the criterion from KWH, in which a particle’s timestep is given by the minimum of $\eta(\epsilon_{\text{grav}}/v)$ and $\eta(\epsilon_{\text{grav}}/a)^{1/2}$, where v is the particle velocity, a is the acceleration, and η is a user-specified number, typically ~ 0.4 .

For the gas particles there is an additional timestep constraint set by the Courant condition (see HK):

$$\Delta t_i = \mathcal{C} \frac{h_i}{h_i |\nabla \cdot \mathbf{v}_i| + c_i + 1.2 (\alpha c_i + \beta h_i |\nabla \cdot \mathbf{v}_i|)}, \quad (7)$$

where $\mathcal{C} \approx 0.3$ is the Courant number and c_i is the sound speed. Particles are binned according to their timestep size into powers-of-two subdivisions of the largest timestep. At any given small timestep each particle falls into one of three categories: (1) “Active”, meaning the given particle needs a recalculation of its force in this small timestep, (2) “Inactive”, meaning the given particle does NOT need recalculation of its force, and (3) “Semi-active” (gas particles only), meaning the particle itself is inactive but it has an SPH neighbor which is active.

To maintain synchronous communication, all processors are assigned the smallest timestep of the entire system. Domain decomposition is not redone, but the locally essential tree is rebuilt and the gravitational force is calculated for all active particles. To compute hydrodynamical forces, data updates are done to allow local advancing of the positions and velocities of Fringe particles. All the smoothing lengths and densities are recalculated, even for inactive particles. Subsequent computations of du/dt and the

acceleration are only performed on active and semi-active particles (required for their scatter contribution to active particles). For inactive particles, all physical quantities are interpolated to be current at each small timestep.

To maintain good load balancing between synchronous communication of these small timesteps, we tally the gravitational work of all active particles at each small timestep and add that to the overall work for that processor. This method is suboptimal since the tree exchange and tree construction overhead remain identical even though there may be only a small number of active particles, but it turns out the load balancing is still reasonable. We leave it for the future to develop a partially asynchronous communication algorithm which may improve load balancing.

3.8. Memory Considerations

Memory considerations are important for the efficiency of a parallel code. By placing the largest possible number of particles on each processor, the amount of time spent performing local computations increases relative to the amount of time spent for computations on remote particles. This means that a relatively smaller amount of remote information is required, and hence overhead for communication time is reduced.

In PTreeSPH, the SPH calculation reuses the memory used to store the N -body tree structure. There are three major uses for memory in the N -body treecode: Storing the particle information, storing the local tree, and storing the locally essential tree information from other processors. The latter two are no longer needed once the gravitational force has been computed, so the memory can be reused to store the Fringe particles and grid-tree structure. PTreeSPH has its own memory handler routines which suballocate the memory out for tree cell storage or SPH storage as required. Thus other than the increased memory required to store the particles' hydrodynamical information (which roughly doubles the amount of memory for particle information), PTreeSPH actually requires no more memory than an N -body version of the code.

On the T3D with 8 Megawords (64 Megabytes) per processor, simulations may run with up to ~ 64 K particles per processor. This is somewhat smaller than ~ 100 K particles per processor possible with the pure N -body treecode, due to the increased memory requirements for SPH information. Currently PTreeSPH is roughly equally limited by memory and time allocation constraints. Newer architectures promise to scale both memory and performance roughly equally, so we anticipate this will continue to be the case in the near future.

3.9. Additions for Cosmological Simulations

PTreeSPH is currently set up to handle periodic boundary conditions, radiative cooling, and heating from a parameterized photoionizing background. We have already described the periodic implementation of the N -body portion of the code in §2.3. For

SPH, the code must detect neighbors on other processors accounting for the periodic nature of the simulation volume. To do this, we first note that domain decomposition does not cut across periodic boundaries, so it is only when Fringe particles are required that periodicity becomes important. Thus periodic boundaries affect SPH only during the building of the LEPL. We utilize the fact that a Fringe particle’s position can be different (in a periodic sense) from the original particle’s position. Whenever a Fringe particle position is received, either during the construction of the LEPL or during a data update, the position of the particle is adjusted to be closest possible to the local domain. Subsequent neighbor finding and SPH computations can then be done with no regard for periodic boundaries. The only difficulty arises when a particle appears multiply in a given processor’s fringe, and such rare cases are detected and Fringe particles are replicated when necessary; in practice this never occurs when the number of processors $N_P \geq 8$.

Radiative cooling and photoionization heating are implemented as described in KWH (§3). Collisional excitation, collisional ionization, recombination, free-free emission and Compton cooling are all included, as well as heating provided by a user-input parameterized ionizing background. Ionization equilibrium is assumed, but not thermal equilibrium. PTreeSPH successfully reproduces the cooling and heating curves shown in KWH figures 1 and 2; the reader is referred there for further details.

Since the cooling timescales can be considerably shorter than the timestep as determined by the Courant condition, the thermal energy cannot be integrated explicitly with the Courant timestep. Instead, we use a Newton-Raphson method to implicitly solve the following equation for $u^{n+1/2}$:

$$f(u^{n+1/2}) \equiv u^{n+1/2} - u^n - \frac{\Delta t}{2}(\dot{u}^{n+1/2} + \dot{u}^n) = 0 \quad (8)$$

where $\dot{u} = \dot{u}_{ad} + \dot{u}_{rad}$ is made up of adiabatic and radiative contributions. The values of u^n and \dot{u}^n are known from the previous step, and $\dot{u}_{ad}^{n+1/2}$ is a stable enough function of $u^{n+1/2}$ to be determined using a predictor-corrector method. On the other hand, $\dot{u}_{rad}^{n+1/2}$ can be a rapidly varying function of $u^{n+1/2}$. Thus the adiabatic portion may be integrated explicitly, but the radiative portion must be integrated implicitly using the Newton-Raphson solver. PTreeSPH’s Newton-Raphson solver brackets the solution, then reduces the acceptable range iteratively until the temperature is determined to an accuracy of one part in 10^{-5} . In cases where a Newton-Raphson iteration would place the solution outside the acceptable range, a bisection iteration is used instead; the algorithm is adapted with extensive modifications from Numerical Recipes (Press et al. 1992). We have found this technique to be quite stable, and requires less computation than integrating $\dot{u}_{rad}^{n+1/2}$ over very small timesteps given by the cooling timescale.

Eventually we plan to add star formation (Katz 1992; Mihos & Hernquist 1994) with feedback. Since each processor is locally self-contained after the LEPL has been built, this addition will be as straightforward as in the serial version of TreeSPH.

4. Testing PTreeSPH

4.1. Spherical Collapse

The collapse of a spherically-symmetric cloud in three dimensions is a good test of a hydrodynamical code’s ability to handle problems with large dynamic range in space and time. Here we compare the results of PTreeSPH to TreeSPH, which in turn agree quite well with one-dimensional finite element calculations of this problem (HK; Evrard 1988). We begin with a self-gravitating gas sphere of radius R and total mass M_T , randomly sampled by 4096 particles with a density profile

$$\rho = \frac{M_T}{2\pi R^2 r}. \quad (9)$$

The gas is initially isothermal with specific energy density $u = 0.05GM_T/R$, and the ratio of specific heats is $\gamma = 5/3$. The artificial viscosity parameters chosen were $\alpha = \beta = 0.5$. The gravitational tolerance parameter was taken to be $\theta = 1.0$ for PTreeSPH, and $\theta = 0.7$ for TreeSPH (which give roughly identical gravitational force accuracies). The gravitational softening length is $0.1R$, and smoothing lengths were varied to keep $N_{\text{smooth}} = 32$ neighbors within a smoothing volume (in the TreeSPH run, there was a tolerance of ± 3 neighbors). The Courant number was taken to be 0.3, and the largest system timestep was taken to be $\Delta t_s = 0.022$ (in the adopted system units of $G = R = M_T = 1$). We do not include radiative processes.

The resulting collapse produces a shock most prominently seen at roughly $t = 0.88$. Figure 3 shows the distribution of density, thermal energy, pressure, and radial velocity as a function of radius. The solid curve is the PTreeSPH result, while the dashed curve is the TreeSPH result. They are quite similar over a dynamic range in density of over 1000, and over a (maximum) dynamic range in time of 32. The shock is resolved over a few smoothing lengths, with no discernible postshock oscillations. Differences are attributable to variations in the gravity implementation and the use of a ± 3 particle tolerance on N_{smooth} in TreeSPH. Results at other times are likewise very similar to TreeSPH results.

This PTreeSPH test was performed on four processors on an SGI Power Challenge. Domain decomposition splits the problem directly through the densest region of the simulation, where smoothing lengths are quite varied. The agreement of the density profile of the two codes down to the lowest radii is evidence that the Fringe particles are being identified correctly (both gather and scatter particles) and all required information is being exchanged appropriately.

4.2. Zel’dovich Pancake

The collapse of a Zel’dovich pancake (Zel’dovich 1970; Bryan et al. 1994) provides an interesting and relevant test for cosmological simulations. The initial conditions are

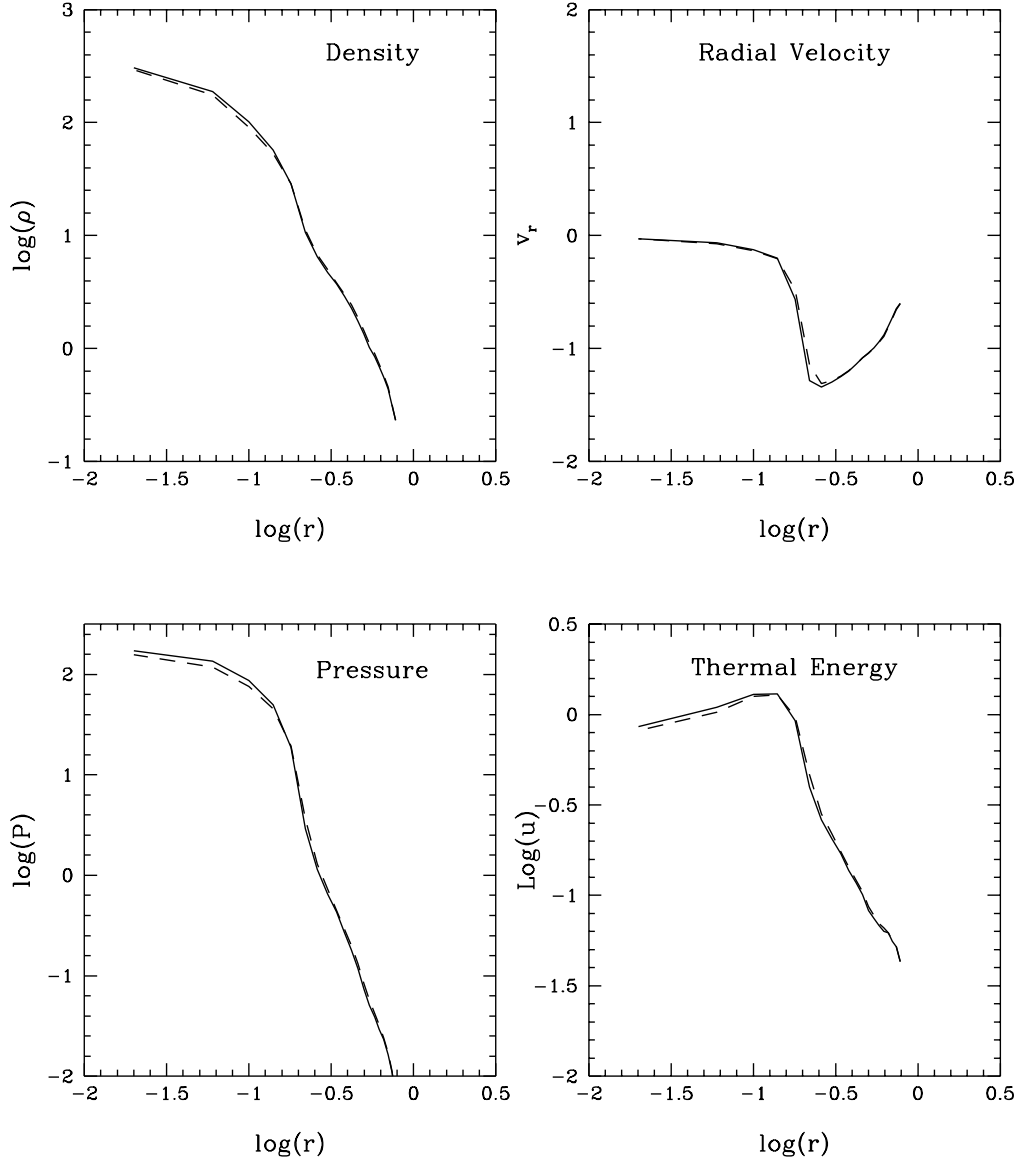


Fig. 3.— Spherical collapse of $\rho \propto 1/r$ sphere at $t = 0.88$, where the infall shock is most clearly visible. The PTreeSPH results (solid line) are quite similar with the TreeSPH results (dashed line), which in turn agree with a 1-D finite difference calculation (see HK). The shock is resolved over two to three smoothing lengths, with no discernible postshock oscillations.

that of a sinusoidal perturbation in velocity and displacement from a lattice. Figure 4 (dotted line) shows T , v_x , and ρ versus x in the initial state at $z = 39$ (the temperature and density plots focus on the central region where the interesting physics occurs at later times). We use 32^3 gas particles (hydrogen fraction by mass $X_H = 0.76$) in an $L = 22.222$ Mpc (comoving) box with $H_0 = 50 \text{ km s}^{-1} \text{ Mpc}^{-1}$, starting at $z = 39$ and ending at $z = 5$. We take $\epsilon_{\text{grav}} = 0.01L$, $\theta = 0.7$, and take large timesteps of $\Delta t = 11.4 \times 10^6$ years. For the hydrodynamics, we set $\gamma = 5/3$, $N_{\text{smooth}} = 32$, $\mathcal{C} = 0.3$, $\alpha = 0.5$ and $\beta = 0.5$. We also set a floor on the smoothing length of $0.25\epsilon_{\text{grav}}$. We include radiative cooling and at late times turn on an ionizing background given by a power law with

$$J(\nu) = 10^{-22}(\nu_L/\nu)F(z) \text{ erg s}^{-1} \text{ cm}^{-2} \text{ sr}^{-1} \text{ Hz}^{-1}, \quad (10)$$

with a redshift dependence

$$F(z) = \begin{cases} 4/(1+z) & \text{for } 3 < z < 6, \\ 1 & \text{for } 2 < z < 3. \end{cases} \quad (11)$$

The simulation was performed on 8 processors of the Cray T3D at the Pittsburgh Supercomputing Center.

The resulting collapse initially follows linear theory, dominated by the gravitational force. The error in v_x during this phase is $\lesssim 0.1\%$. The gas cools adiabatically from 10^4 K due to cosmological expansion, with slight variations due to differences in density.

After the caustic forms, hydrodynamical effects become dominant and a central shock region develops, as shown by the short dashed lines in Figure 4 ($z = 12$ at this time). Radiative processes efficiently cool the outer shock envelope, so the temperature in the entire shock region is maintained at $T \approx 10^{4.2}$ K. As the shock strength builds, the characteristic dual-shock pattern emerges, as shown by the state of the system at $z = 9$ in Figure 4 (long dashed line), while the region between the shock fronts remains at $T \approx 10^{4.2}$ K due to radiative cooling. Figure 4 (solid line) shows the final state at $z = 5$, where a more complicated structure has developed due to secondary infall and resultant shock heating. The background gas is heated by the ionizing background to $T \approx 10^{4.5}$ K, where heating, radiative cooling, and adiabatic cooling due to cosmological expansion are in equilibrium.

While there are no analytical predictions for this problem in the nonlinear regime, the general features are in good agreement with expectations in a problem where shock heating, radiative cooling, and photoionization all play major roles in governing the evolution of the system.

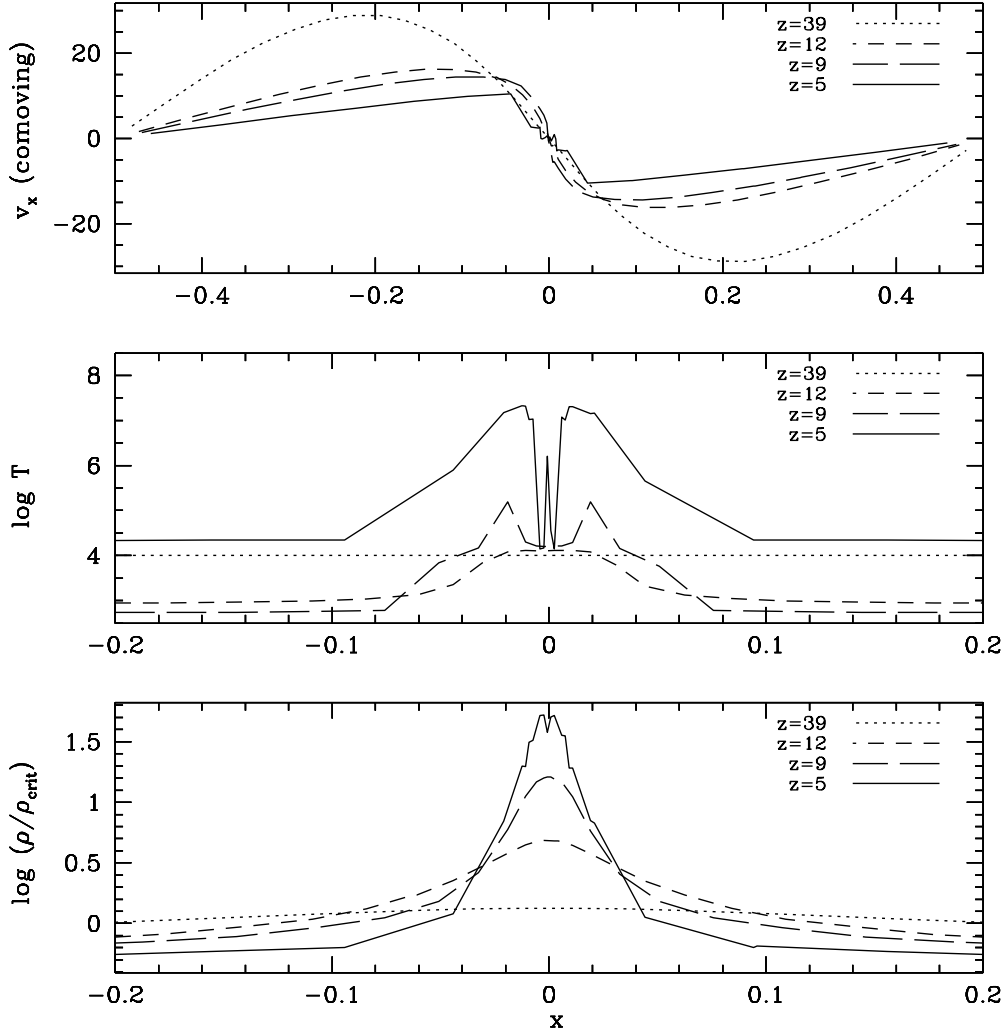


Fig. 4.— Zel’dovich pancake collapse of a sheet of gas showing the x -direction velocity, temperature and density binned along the x -axis. Dotted line shows initial state at $z = 39$, a sinusoidal perturbation in displacement and velocity. Short dashed line shows the state at $z = 12$, as the initial shock has formed. Long dashed line shows the state at $z = 9$, showing the dual-shock front pattern with the central region maintained at $10^{4.2}$ K by radiative cooling. The final state at $z = 5$ is shown as the solid line, with multiple shocks due to secondary infall and the background gas heated due to photoionization.

4.3. Cosmological Simulation: Comparison With TreeSPH

As a final test, we redid the TreeSPH simulation described in Weinberg, Hernquist & Katz (1997) using PTreeSPH. This is a cosmological simulation of the Standard Cold Dark Matter (CDM) model with $\Omega = 1$, $H_0 = 50 \text{ km s}^{-1} \text{ Mpc}^{-1}$, $\Omega_b = 0.05$, and $\sigma_{16, \text{mass}} = 0.7$, in a 22.222 Mpc (comoving) cube with 32^3 dark matter and 32^3 gas particles. The ionizing background used is given in equation (10). The simulation was started at $z = 49$ and run to $z = 2$, using 762 large timesteps of $\Delta t = 3.3 \times 10^6$ years, with small timesteps as low as $\Delta t/4$ (timesteps down to $\Delta t/16$ were allowed but never required). We took $\epsilon_{\text{grav}} = 20 \text{ kpc}$ and set a floor on the SPH smoothing length of 5 kpc. Other SPH and cooling parameters were taken to be the same as in the Zel’dovich pancake test. We performed this run on 16 processors of the Cray T3D at Pittsburgh Supercomputing Center.

Figure 5a (top panel) shows a scatter plot of density (in units of the mean baryonic density) vs. temperature for all gas particles in the simulation at $z = 2$. The particles fall into three main categories, as described in KWH: Low-density gas cooled adiabatically by cosmic expansion; overdense, shock-heated gas which generally surrounds large halos; and high-density gas which has radiatively cooled to $T \sim 10^4 \text{ K}$ and lies in dense clumps. The last group is what we associate with galaxies.

Figure 5b shows the same scatter plot for the identical TreeSPH run, reproduced from Figure 3 of Weinberg, Hernquist & Katz (1997). While most general features are similar, there is a noticeable difference in the number of particles lying in cold, collapsed clumps, particularly of intermediate density ($\rho \gtrsim 10^3$). This arises because TreeSPH systematically overestimates accelerations in the linear phase as described in § 2.3, hence it heats gas at an earlier time and prevents the early formation of small collapsed objects. This early heating was very pronounced in a comparison of TreeSPH and PTreeSPH runs of the Zel’dovich pancake test described above: TreeSPH produced an initial shock at $z \approx 15$, while PTreeSPH produced an initial shock at $z \approx 11$. Comparisons of ρ vs. T plots for this cosmological simulation at various redshifts also showed more hot particles in the TreeSPH run at early times. PTreeSPH handles the linear regime more accurately by including quadrupole Ewald terms and using a smaller tolerance parameter at early times. Despite the difference in dense particles, visualization showed that the major structures formed in the PTreeSPH and TreeSPH runs are all very similar.

Another difference from Figure 5 is that the reservoir of low-density, photoionization-heated gas shows less scatter in the PTreeSPH run than in the TreeSPH run. The difference likely arises from the accuracy of the Newton-Raphson solvers implemented in the two code. The temperature of a given SPH particle depends on the thermal energy and the electron density, but the electron density in turn depends on the temperature through the cooling and heating rates. Thus at every iteration of the Newton-Raphson solver, the mutual dependence of T and n_{elec} must be iterated until a

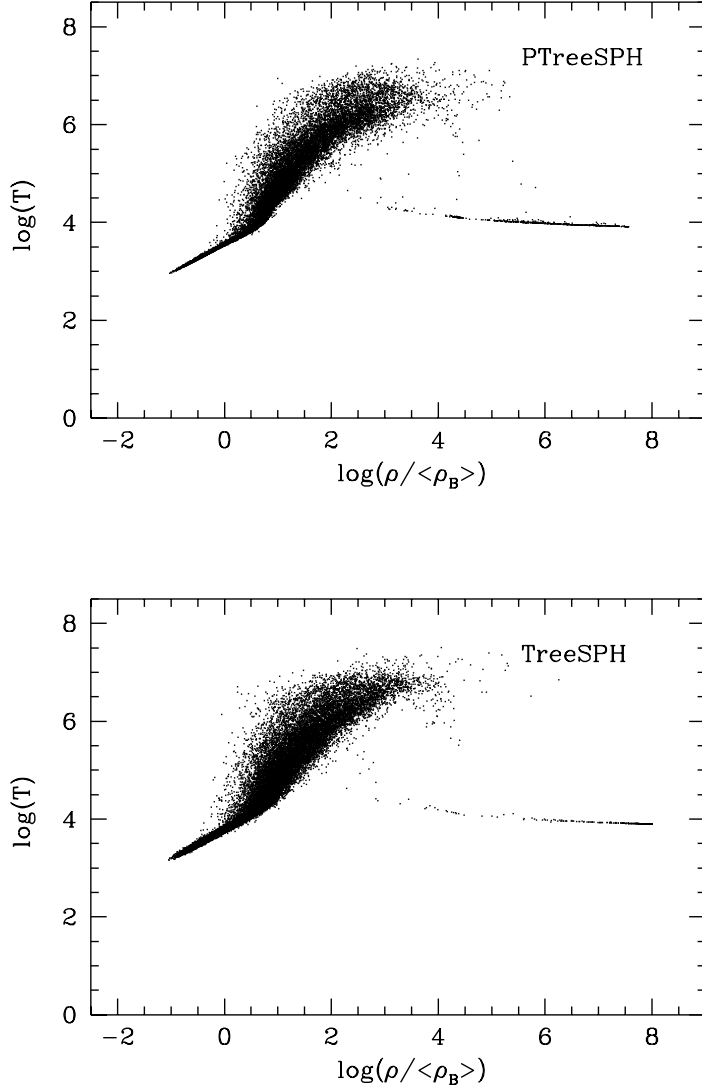


Fig. 5.— Scatter plot showing density ρ vs. temperature T for every SPH particle in the 2×32^3 run described in 4.3. Top panel shows PTreeSPH results, bottom panel shows TreeSPH results. Both codes show a reservoir of underdense cool gas heated by photoionization, a reservoir of shock-heated gas of moderate density, and a cool high-density component corresponding to collapsed objects. The last component shows some differences between the two codes, with PTreeSPH having more particles in collapsed objects. This arises from systematic overestimation of acceleration in the linear regime with TreeSPH, causing more shock heating at early times which delays the initial formation of small clumps.

convergent solution is achieved. In TreeSPH, only one iteration is used; however, this is sometimes insufficient to achieve convergence, especially in the low-density regime where heating is sensitively balanced by adiabatic cooling from cosmological expansion. PTreeSPH iterates until convergence to obtain a tighter solution for the temperature in this regime.

5. Performance Characteristics of PTreeSPH on a Cray T3D

5.1. Timing Results

For benchmarking purposes, we ran the cosmological simulation with 64^3 dark matter and 64^3 gas particles described in KWH (similar to the one in the previous section except with eight times as many particles), beginning at $z = 2$ and continuing for ten large timesteps. At $z = 2$, the simulation is already quite clustered and uses eight small timesteps per large timestep, so these benchmarks actually represent those for 80 steps. We ran on eight processors of the Cray T3D at the Pittsburgh Supercomputing Center. This run is optimized to have the most number of particles per processor (64K) that memory constraints will allow.

We divide the simulation into six main routines which take up nearly all the computation time:

1. Gravity parallel overhead, which includes domain decomposition and locally essential tree building,
2. Gravity force calculation, which includes local tree building,
3. LEPL Building,
4. Data Updates,
5. Smoothing Length Adjustment, and
6. Hydrodynamical force calculation, which includes neighbor finding.

	Ave Time (sec)	% Time	Load Balancing	Scalability
Total	3929.1	100.0	89.6	86.9
Gravity Parallelization	15.3	0.4	99.5	62.6
Gravity Force	1288.3	32.8	95.8	96.0
LEPL Building	134.6	3.4	97.2	62.6
Data Updates	261.5	6.7	64.5	62.6
h_{smooth} Adjustment	423.7	10.8	85.4	88.9
SPH Force	1333.9	33.9	88.7	88.9

Table 5.1: Benchmarks for 2×64^3 run averaged over ten large timesteps. Load balancing is defined in equation (12), and scalability is described in §5.3.

Table 5.1 shows the wallclock time taken per timestep per processor, averaged over ten large timesteps, along with the corresponding fraction of the total computational time for each of the six routines. The gravity and SPH computations each take about one-third of the total time, with the rest divided among parallel overhead and smoothing length adjustment. About 12% of the total time is not accounted for, which represents I/O and initialization times. The parallel overhead for the gravity computation is negligible, but for SPH it takes $\sim 10\%$ of the total time. Much of this time goes into determining which particles need to be exchanged, rather than interprocessor communication. In addition, the exchange of Fringe particle information must be done over every pair of processors, making this is N_P^2 process (where N_P is the number of processors), rather than an $N_P \log N_P$ process as for the gravity parallelization (see Paper I). Despite these difficulties, the parallel overhead is still quite reasonable, as roughly 90% of the time is spent performing useful computations.

The average wallclock time taken per step with eight processors is around 3900 secs, or a little over an hour per large timestep (*i.e.* eight small timesteps). This translates to roughly 9 node-hours per large timestep for this 2×64^3 simulation. To evolve from $z = 49$ to $z = 2$ (*i.e.* the simulation done in KWH) requires 762 large timesteps. Since the early part of the simulation runs faster (fewer small timesteps), we conservatively estimate that this simulation could be run in 6000 node-hours of a Cray T3D. A simulation with 10^7 particles and half the resolution would conservatively require 32 times as much time, which on a Cray T3E (approximately 4 times faster than a T3D) translates to roughly 50,000 node-hours. Alternatively, a 2×10^6 particle simulation may be run to $z = 0$ in around the same time. Note that these benchmarks represent conservative values based on incorporating cooling (which increases the SPH time by up to a factor of two) and periodic boundary conditions (which increases the overall code time by roughly a factor of two). Simulations not requiring these effects would be considerably faster, as would simulations which require fewer small timesteps (*e.g.* less clustered or lower resolution simulations).

5.2. Load Balancing

Ideally, a code should divide the computational work equally among all processors. However, because it is difficult to estimate the workload *a priori*, some fraction of the time will be spent idly waiting for the processor with the largest workload to complete its computations. Such idle time occurs whenever an exchange of information is required, since all processors must be synchronized to perform exchanges in PTreeSPH’s synchronous communication scheme. The six routines listed in the previous section divide the computation into blocks between required exchanges.

We measure load balancing in each routine by computing the fractional amount of time spent idle while another processor performs computations. More specifically, if

t_{\max} is the time taken by the processor with the most work for a given routine, and t_i is the time taken by processor i , the load balancing for that routine is given by

$$L = \frac{1}{N_{\text{procs}}} \sum_{i=1}^{N_{\text{procs}}} 1 - (t_{\max} - t_i)/t_{\max} \quad (12)$$

Table 5.1 shows the load balancing for each of the six routines, averaged over the 10 timesteps. The gravity computation is load balanced at roughly a 96% level, the SPH computation is around 89%, and the smoothing length adjustment is around 85%. The data update routine is the only one which does not load balance well (64%), but since the time in this routine is fairly small, it does not significantly degrade the overall performance. Overall, the code is load balanced at roughly a 90% level, meaning that only 10% of the wallclock time is spent with processors idle. While these are not optimal values, they are quite reasonable considering that the domain decomposition scheme is designed to load balance the gravity portion only. An asynchronous communication scheme may improve load balancing, but the increased complexity of the code may prove detrimental to the overall performance. We leave this for future investigations.

5.3. Scalability

Ideally, the speed of each routine should scale linearly with the number of processors. However, due to irregular domain sizes and increasing communication overhead, the speed degrades with increasing numbers of processors. To test this, we consider 10-timestep runs as described above with 8, 16, 32 and 64 processors. Figure 6 shows the scaling with number of processors for three major components of the code: the gravity portion, the SPH portion (which here includes smoothing length adjustment), and the LEPL portion (which here includes data updates). The last column of Table 5.1 shows the scaling as a percentage of ideal between 8 and 16 processors.

The gravity portion scales very well all the way from 8 to 64 processors, suffering just a few percent loss of speed at each increment. The SPH portion does not scale nearly as well out to 64 processors; however, between 8 and 16 processors, the loss is only $\sim 11\%$ from ideal. The parallelization overhead stays roughly constant. Overall, PTreeSPH’s scaling is dominated by the SPH portion, but between 8 and 16 processors the loss of speed is only $\sim 14\%$. The scaling of ultimate interest is that between eight and one processors, which we cannot directly measure, but we take the scaling between 16 and 8 processors as a conservative estimate. These graphs illustrate the importance of minimizing the number of processors used for a given simulation. As memory constraints are alleviated in future machines, the scalability of PTreeSPH should improve.

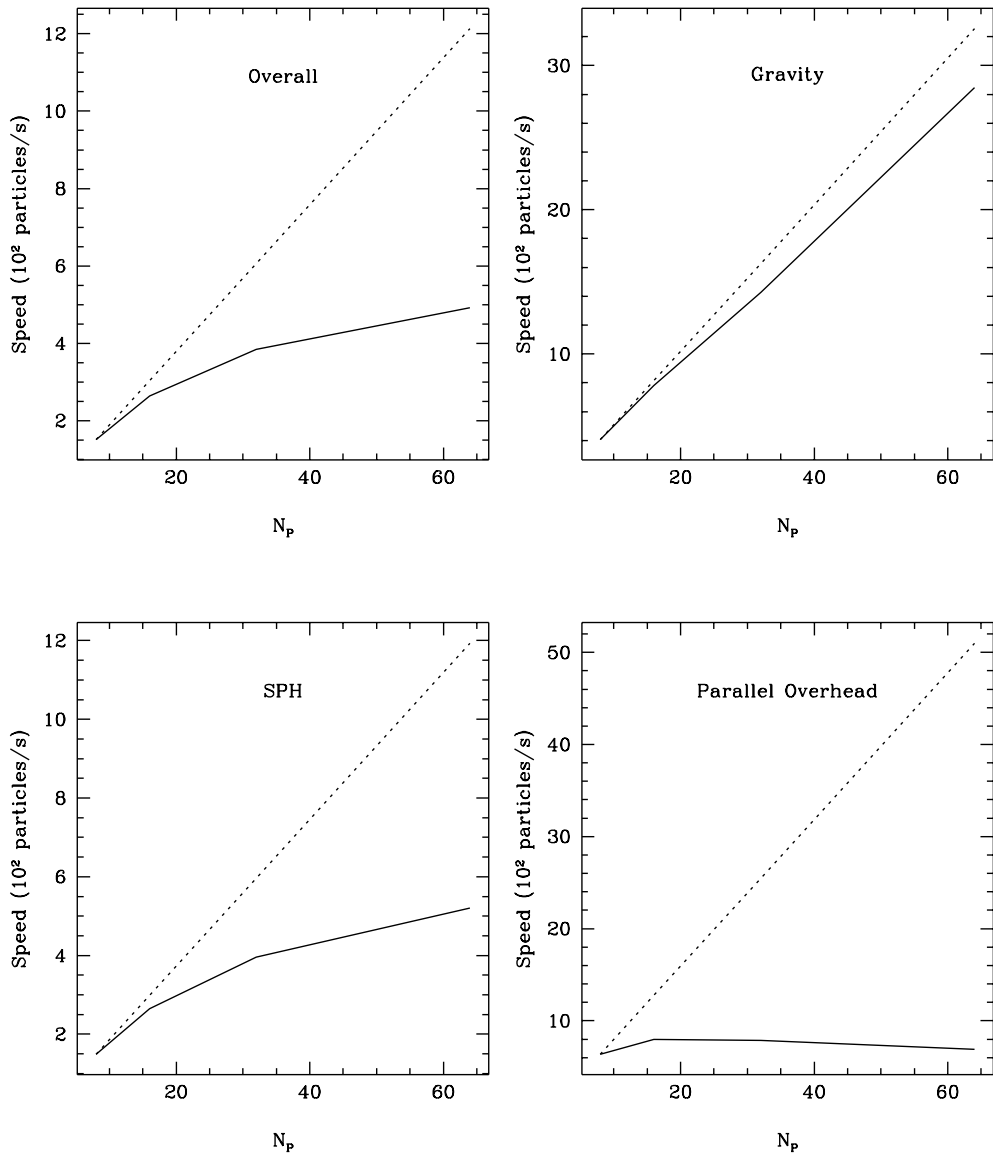


Fig. 6.— Scalability of various routines of PTreeSPH with number of processors, for the run described in §5.3. Solid lines represent PTreeSPH timings at 8, 16, 32 and 64 processors. Dotted lines show ideal scaling from 8 processors. Upper left shows the overall code scaling. Upper right shows the gravity portion scaling, which is quite good. Lower left shows scaling of the SPH portion, including smoothing length adjustment. This is fairly poor up to 64 processors, but reasonable up to 16 processors. Lower right shows the scaling of the parallelization routines, the domain decomposition, locally essential tree building, LEPL building and data updates. This speed remains as a fairly constant overhead for any number of processors. The SPH and parallelization scaling illustrates the efficiency gained by minimizing the number of processors used for a given simulation.

6. Summary and Future Work

A parallel TreeSPH code for performing cosmological hydrodynamical simulations has been presented. The physics is incorporated in a manner quite similar to the TreeSPH code (HK; KWH), but the algorithm has been redesigned to handle difficulties unique to the massively parallel environment. The code is capable of performing cosmological simulations in a periodic volume, including the effects of radiative cooling and heating from a parameterized ionizing background. The use of massively parallel supercomputers currently enables one to perform simulations with roughly an order of magnitude more particles than is practically possible on a vector supercomputer. Moreover, with the current rate of advance in chip technology, the massively parallel approach promises to provide rapid further increases in computational power and therefore simulation size. Currently, a cosmological hydrodynamical simulation of 10^7 particles down to $z = 2$ is feasible within a typical allocation of supercomputer time; alternatively, one can explore models with many smaller simulations. Significantly larger simulations are possible for applications which do not require periodic boundaries, or whose matter is less clustered than in a cosmological simulation.

PTreeSPH has been implemented with primary concern for portability and expandability, and secondary concern for optimal efficiency. Nevertheless, the code achieves good load balancing ($\sim 90\%$) and has fairly low communication overhead ($\sim 10\%$). Compile-time flags have been implemented to easily include or exclude various physical processes such as hydrodynamics, cooling, and cosmology. The use of the MPI message passing software allows for easy portability between parallel platforms; already the code has been run successfully on the Cray T3D, the IBM SP2, and an SGI Power Challenge. The building of locally essential problems, both for gravity and hydrodynamic forces, allows for straightforward incorporation of other physical processes as desired. Together with its fully Lagrangian nature, this will make PTreeSPH useful for a wide variety of astrophysical applications, including cosmology, galaxy interactions and cluster formation.

7. Acknowledgements

We are grateful to Neal Katz, David Weinberg and Guohong Xu for helpful comments and suggestions. We acknowledge grants of computer resources by Pittsburgh Supercomputing Center and the Cornell Theory Center. This work was supported by the Grand Challenge Cosmology Consortium, NSF grant ASC 93-18185, and the Presidential Faculty Fellows Program.

REFERENCES

- Aarseth, S. J. 1985 in Proc. Dynamics of Star Clusters, Dordrecht: D. Reidel Publishing, p. 251
- Barnes, J. & Hut, P. 1986, Nature, 324, 446 [BH]
- Barnes, J. 1994, in Computational Astrophysics, eds. J. Barnes et al. (Berlin: Springer-Verlag)
- Bryan, G. L., Cen, R., Norman, M. L., Ostriker, J. P. & Stone, J. M., 1994, ApJ, 428, 405
- Bryan, G. L. & Norman, M. L. 1995, BAAS, 187, 95.04
- Colella, P. & Woodward, P. R. 1984, J. Comp. Phys., 54, 174
- Couchman, H. M. P., Thomas, P. A. & Pearce, F. R. 1995, ApJ, 452, 797
- Dikaiakos, M. D. & Stadel, J. 1997, in preparation, <http://www-hpcc.astro.washington.edu/papers/marios/perform/perform.html>
- Dubinski, J. 1996, NewA, 1, 133
- Dubinski, J. 1997, in preparation
- Efstathiou, G., Davis, M., Frenk, C. S. & White, S. D. M. 1985, ApJS, 57, 241
- Evrard, A. E. 1988, MNRAS, 235, 911
- Ewald, P.P. 1921, Ann. Physik., 64, 253
- Gammie, C. F. 1992, Ph.D. Thesis, "The Formation of Giant Molecular Clouds", Princeton University
- Gingold, R. A. & Monaghan, J. J. 1977, MNRAS, 181, 375
- Hernquist, L. 1987, ApJS, 64, 715
- Hernquist, L. & Katz, N. 1989, ApJS, 70, 419 [HK89]
- Hernquist, L. 1990, J. Comp. Phys., 87, 137
- Hernquist, L., Bouchet, F.R. & Suto, Y. 1991, ApJS, 75, 231 [HBS]
- Hernquist, L. & Ostriker, J. P. 1992, ApJ, 400, 460
- Hernquist, L., Katz, N., Weinberg, D. H. & Miralda-Escudé 1996, ApJ, 457, L51
- Heyl, J. S., Cole, S., Frenk, C. S. & Navarro, J. F. 1995, MNRAS, 274, 755
- Hockney, R. W. & Eastwood, J. W. 1980, Computer Simulation Using Particles (New York: McGraw-Hill)
- Jenkins, A., Frenk, C. S., Pearce, F. R., Thomas, P. A., Hutchings, J., Colberg, M., White, S. D. M., Couchman, H. M. P., Peacock, J. A., Efstathiou, G. P. & Nelson, A. H. 1996, to appear in M. Persic and P. Salucci, eds., Dark and Visible Matter in Galaxies, PASP Conference Series, astro-ph/9610206

- Kang, H., Ostriker, J. P., Cen, R., Ryu, D., Hernquist, L., Evrard, A. E., Bryan, G. L., & Norman, M. L. 1994, *ApJ*, 430, 83
- Katz, N. & Gunn, J. E. 1991, *ApJ*, 377, 365
- Katz, N. 1992, *ApJ*, 391, 502
- Katz, N. & White, S. D. M. 1993, *ApJ*, 412, 455
- Katz, N., Weinberg, D. H. & Hernquist, L. 1996, *ApJS*, 105, 19 [KWH]
- Kauffmann, G. & White, S. D. M. 1993, *MNRAS*, 261, 912
- Kundic, T., Spergel, D. & Hernquist, L. 1993, *BAAS*, 183, 87.08
- Lucy, L. 1977, *AJ*, 82, 1013
- Mihos, J. C. & Hernquist, L. 1994, *ApJ*, 437, 611
- Monaghan, J. J. 1992, *ARA&A*, 30, 543
- Monaghan, J. J. & Lattanzio, J. C. 1985, *A&A*, 149, 135
- Pearce, F. R., Couchman, H. M. P., Jenkins, A. R. & Thomas, P. A. 1995, “Hydra – Resolving a Parallel Nightmare”, in *Dynamic Load Balancing on MPP systems*, <http://star-www.maps.susx.ac.uk/frp/virgo/hydra-par.ps.gz>
- Pen, U. 1995, *ApJS*, 100, 269
- Press, W. H., Teukolsky, S. A., Vetterling, W. T. & Flannery B. P. 1992, *Numerical Recipes in C* (Cambridge: Cambridge University Press)
- Ryu, D., Ostriker, J. P., Kang, H. & Cen, R. 1993, *ApJ*, 414, 1
- Salmon, J. 1991, Ph.D. Thesis, “Parallel Hierarchical N-Body Methods”, California Institute of Technology
- Somerville, R. et al. 1997, in preparation
- Steinmetz, M. 1996, *MNRAS*, 278, 1005
- Villumsen, J. V. 1989, *ApJS*, 71, 407
- Warren, M. S. & Salmon, J. K. 1994, Los Alamos National Lab internal report, <http://qso.lanl.gov/papers/cpc/v9.ps>
- Weinberg, D. H., Hernquist, L. & Katz, N. 1997, *ApJ*, submitted
- Xu, G. 1995, *ApJS*, 98, 355
- Xu, G. 1997, *MNRAS*, in press
- Zel’dovich, Y. B. 1970, *AA*, 5, 84